Statistical analysis of excitation functions for $^{28}Si+^{28}Si$ elastic scattering and reactions

S. Saini and R. R. Betts
Chemistry Division, Argonne National Laboratory, Argonne, Illinois 60439
(Received 19 December 1983)

Angle integrated excitation functions for elastic scattering and reactions of $^{28}Si+^{28}Si$ have been measured in 100 keV steps over the energy range $E_{lab}=105-121$ MeV. Narrow fluctuations are observed in all channels as well as in the angle-integrated cross section summed over all channels. These data have been subjected to a detailed statistical analysis. The probability densities of the summed deviation and cross-correlation functions have been derived from the assumptions of the statistical model and compared with the experimental results. These statistical tests show that the observed narrow structures are of nonstatistical character and correspond to long lived states of the composite system with high angular momenta and excitation energy.

I. INTRODUCTION

Since the first observation of resonance phenomena[1] in excitation functions for the $^{12}C+^{12}C$ system at sub-Coulomb energies, tremendous effort has been made[2-10] to try and gain a clear understanding of this phenomenon, both experimentally and theoretically. Resonance phenomena in heavy-ion reactions present many interesting questions which concern not only the mechanisms of heavy-ion reactions, but also questions of the nuclear structure of the composite system at high excitation energies and high angular momenta. One of the earliest features noted was that the intermediate structure resonances were observed only in systems where the number of open channels and the level density in the compound nucleus are small, and at least one of the nuclei in the entrance channel was C or O. Most studies[2-9] have therefore been carried out for systems where at least one of the reaction partners is C or O. It is only recently that the detailed measurements on much heavier systems such as $^{28}Si+^{28}Si$ (Refs. 10 and 11) have been reported. Contrary to earlier beliefs, this system shows[10] resonance phenomena similar to that observed in light systems.

Theoretical discussions of all these data in terms of the band crossing model,[12] the double resonance mechanism,[13] the coupled channel model,[14] the barrier top model,[15] and the doorway state model,[16] have attempted to explain the origin of these structures. Although some of these models give a reasonable account of the gross features of the experimental data, there is still no definitive understanding of the microscopic nuclear structure underlying the observed narrow structures.

In order to gain a better understanding of the reaction mechanism and the nature of the structural features of the intermediate structures, measurement of excitation functions in fine energy steps and for several different exit channels are necessary. In the energy regime where intermediate structures are observed, however, nonresonant processes may contribute a large fluctuating background. The data must therefore be subjected to critical tests in order to distinguish true resonance structures from nonresonant fluctuations.

Some of the features of $^{28}Si+^{28}Si$ interactions have been recently investigated by Betts *et al.*[10,11] These measurements[10] were made using a fairly thick target and in 1 MeV steps. In order to investigate the observed structures in more detail, these data were remeasured using thin targets and in much smaller energy steps. The excitation functions for five different exit channels were measured in 100 keV steps over an energy range of 105–121 MeV. Since correlations between different channels are the most sensitive signature for discriminating between true resonance structures and fluctuations, the data have been analyzed using summed deviation and cross correlation functions.[8] These two methods are best suited for searching for correlations among different channels. To establish the nonstatistical character of the observed structures conclusively, the statistical confidence limits were calculated using the derived probability densities for the summed deviation and cross correlation function. The statistical tests therefore determine whether the excitation functions are inconsistent with the statistical model and thus locate nonstatistical structures.

These data and a preliminary version of the results of the statistical analysis have been reported in Ref. 17. This paper contains an expanded discussion of the experimental measurements and a detailed presentation of the statistical analysis. The experimental measurements and the results are described in Sec. II and the statistical analysis is presented in Sec. III. Section IV contains a discussion of the results of the analysis and the conclusions.

II. EXPERIMENTAL METHOD AND RESULTS

A ^{28}Si beam from the Brookhaven National Laboratory MP tandem was used to bombard a target consisting of 7 $\mu g/cm^2$ Si metal evaporated on a 20 $\mu g/cm^2$ C backing. The target was mounted with the ^{28}Si toward the beam and corresponded to a beam energy loss of ~ 70 keV (lab) over the energy range of the experiment. The elastic and inelastic events were detected using a kinematic coincidence arrangement consisting of two large area (600 mm^2) Si surface barrier detectors placed on either side of the beam axis. The defining detector covered the angular

range 33.5°—47.5° in the reaction plane with a solid angle of 60 msr. The recoil detector on the other side of the beam axis subtended a 2° larger range in both the horizontal and vertical planes. The coincidence efficiency of this arrangement is close to 100% for the elastic scattering and decreases almost linearly to zero for two-body inelastic events with $Q=-20$ MeV. A detector placed at 15° with respect to the beam direction was used to monitor the elastic scattering for the purpose of normalizations. The energy signals from the defining (E_D) and recoil (E_R) detector were summed to provide a total energy signal ($E_T=E_D+E_R$). For two-body final states, E_T is independent of the scattering angle and was used to generate a Q value spectrum ($Q=E_T-E_I$, where E_I is the beam energy). Data were taken in 100 keV steps over the bombarding energy range of 105—121.1 MeV. The data were normalized both with respect to the integrated beam current and to the elastic yield in the monitor detector. Many repeat points taken throughout the experiment verified the accuracy of these procedures.

A typical Q value spectrum obtained at a bombarding energy of 110 MeV is shown in Fig. 1. The identification of the resolved peaks in Fig. 1 is based on the results of the previous[11] high resolution study. Yields for the elastic, single 2^+, mutual $(2^+,2^+)+4^+$, mutual $(4^+,2^+)$, and the yield in the spectrum (REST) above the mutual $(4^+,2^+)$ ($-7.5\leq Q\leq -20$ MeV) as well as the total yield ($0\leq Q\leq -20$ MeV) in the spectrum were extracted at each bombarding energy. The yields for the resolved peaks were obtained from fits to the appropriate region of the spectrum using four Gaussian peaks with fixed

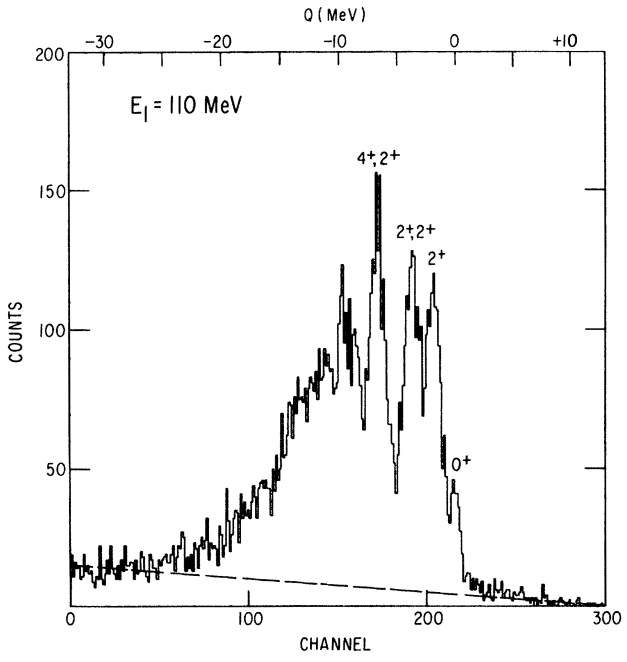

FIG. 1. Q value spectrum for coincident fragments obtained at a bombarding energy of 110 MeV. The elastic, 2^+, unresolved mutual $(2^+,2^+)+4^+$, and the mutual $(4^+,2^+)$ peaks are labeled. The dashed line indicates a background which was subtracted from the spectrum.

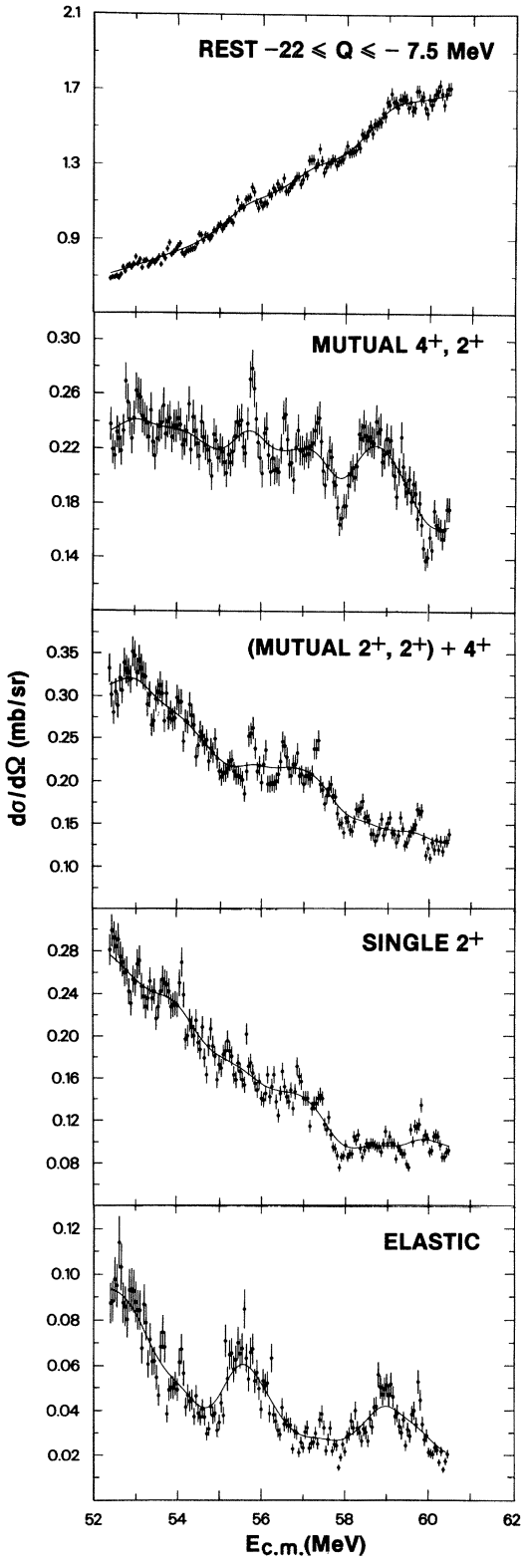

FIG. 2. Angle averaged cross sections for the elastic, 2^+, $(2^+,2^+)+4^+$, $(4^+,2^+)$, and REST shown plotted as a function of center-of-mass bombarding energy. The solid lines are the cross sections obtained from the data using a Gaussian smoothing function with FWHM 1.5 MeV.

widths. To the extent that the experimental peak shapes are accurately described by Gaussians, this procedure removes the possibility that spurious correlations can be introduced as a result of imperfect resolution of these peaks. The angle averaged excitation functions for elastic, single 2^+, mutual $(2^+,2^+)+4^+$, mutual $(4^+,2^+)$ and "REST" are shown in Fig. 2, and for the "TOTAL" in Fig. 6(a). The uncertainties in the relative cross sections estimated from the reproducibility of the repeat points and statistics are less than 5% with the exception of the elastic channel which had poorer statistics and an error of 10%. The absolute cross sections are, however, somewhat more uncertain, due largely to uncertainties in the corrections for the efficiency of the coincidence arrangement.

The excitation functions in Fig. 2 and Fig. 6(a) show two distinct types of structures, broad structures of width $\Gamma_{\text{c.m.}} \simeq 2.0$ MeV, each of which is fragmented into several much narrower structures of width $\Gamma_{\text{c.m.}} \simeq 150$ keV. The overall features of the present data are in good agreement with the results of an earlier measurement[10] with a much thicker target and larger energy steps. The present data with fine energy steps, however, reveals a much richer structure than was evident in the earlier data.[10] Many of the narrow structures appear to be strongly correlated in all the channels, a feature which is not expected for structures arising from statistical fluctuations. However, the data have to be subjected to the critical tests of statistical fluctuation analysis before any conclusions as to the nonstatistical nature of these structures can be drawn. The statistical analysis of the present data will be discussed in detail in the next section.

III. ANALYSIS

The identification of intermediate structure resonances in the presence of a possibly fluctuating background is one of the long-standing problems in nuclear physics. Several types of statistical tests have been suggested in the literature[8,18,19] to distinguish the resonance structures from statistical fluctuations, the most critical and effective test of which are those which search for correlations between different channels, e.g., the method[8,19] of (i) energy dependent deviation functions, (ii) cross correlation functions, and (iii) counting the number of correlated maxima. Before ascribing a nonstatistical nature to a structure observed in the deviation or cross correlation function, the statistical significance limits must be calculated for these quantities. Though methods (i) and (ii) have been widely used in the literature, confidence limits have not, in general, been calculated for these quantities. Recently Lang *et al.*[20] have calculated the statistical significance for deviation functions. In method (iii) the probability of observing a correlated maxima in m excitation functions is simply given by a binomial distribution and can be calculated easily. This method, however, suffers from the drawback that the binomial parameter in the distribution function changes with different definitions for the existence of a maximum in the measured excitation function.

Let us denote the differential cross sections in different channels by $\sigma_k(E)$, $k=1,2,\ldots,M$. To perform the statistical tests, the average cross section $\langle\sigma_k(E)\rangle$ was generated by a sliding average using a Gaussian smoothing function of FWHM=1.5 MeV. The average cross sec-

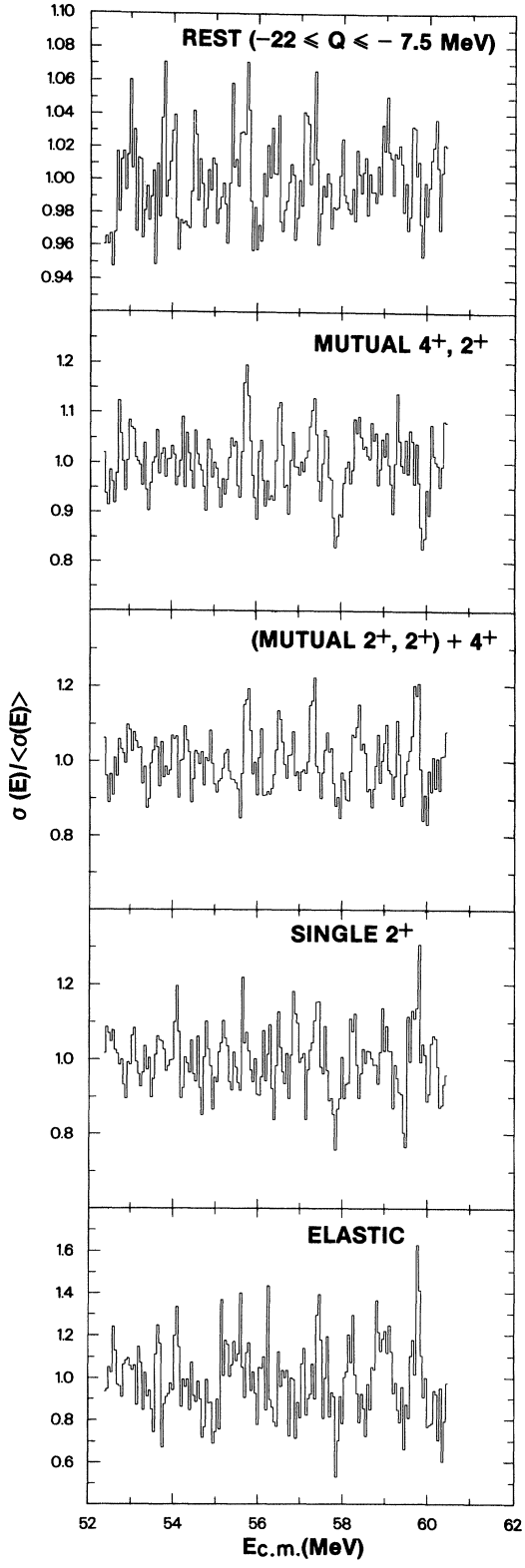

FIG. 3. The ratio $\sigma_k(E)/\langle\sigma_k(E)\rangle$ shown plotted as a function of center-of-mass bombarding energy for the five channels.

tions obtained this way are shown by the solid curves in Fig. 2. We find that though the averaging has removed the narrow structures, the broad structure still persists. To remove the broad structures, we generate a new excitation function

$$Y_k=\sigma_k(E)/\langle\sigma_k(E)\rangle$$

for each channel. The new excitation functions Y_k for each channel are shown in Fig. 3. It has been shown that the probability density of Y_k is given by[21–23]

$$P(Y_k)=\frac{N_k}{1-Y_{D_k}}\left[\frac{Y_k}{Y_{D_k}}\right]^{(N_k-1)/2}\exp[-N_k(Y_k+Y_{D_k})/(1-Y_{D_k})]I_{N_k-1}[2N_k(Y_kY_{D_k})^{1/2}/(1-Y_{D_k})]\,, \tag{1}$$

where N_k is the number of independent channels[23] in the reaction, Y_{D_k} is the nonfluctuating or "direct" contribution to the average cross section, and I_N is a modified Bessel function of order N. The autocorrelation function $R_k(\epsilon)$ is defined as

$$R_k(\epsilon)=\left\langle\!\!\left\langle\left[\frac{\sigma_k(E)}{\langle\sigma_k(E)\rangle}-1\right]\left[\frac{\sigma_k(E+\epsilon)}{\langle\sigma_k(E+\epsilon)\rangle}-1\right]\right\rangle\!\!\right\rangle\,, \tag{2}$$

where $\langle\langle\ \rangle\rangle$ now denotes the averaging over the whole energy range of the excitation function. The normalized variance is given by

$$R_k(0)=R_k(\epsilon=0)=\frac{1}{N_k}(1-Y_{D_k}^2)\,, \tag{3}$$

and, given N_k, can be used to deduce the value of Y_{D_k}. The value of N_k, the effective number of channels for a given transition, can vary with angle; ranging in the present case from $N_k=1$ at 0° and 180° to $N_k^{\max}=g/2$ (g even) or $(g+1)/2$ (g odd), where $g=(2I_1+1)(2I_2+1)$ and I_1,I_2 are the spins of the final fragments. In practice, we find that the calculated probability densities do not depend sensitively on the particular values of N_k and Y_{D_k} providing Eq. (3) is satisfied with $R_k(0)$ equal to the experimental values. The values of Y_{D_k} obtained using various values of N_k are listed in Table I and those labeled "Mean" were used to generate the theoretical probability distributions which are used to compare with the experimental results.

The deviation function for each channel is defined as,

$$D_i(E)=\frac{Y_i-\langle\langle Y_i\rangle\rangle}{(\langle\langle Y_i^2\rangle\rangle-\langle\langle Y_i\rangle\rangle^2)^{1/2}}\,. \tag{4}$$

The statistical model probability distributions for $D_i(E)$ can be calculated using Eq. (1). The advantage of defining $D_i(E)$ in this way is that both the experimental and theoretical distributions of $D_i(E)$ are expected to be approximately normally distributed with mean and variance of 0 and 1, respectively. The experimental frequency distribution of $D_i(E)$ and their statistical model predictions are shown in Fig. 4. The standard normally distributed probability functions are also shown in Fig. 4 for comparison. We find that the theoretical predictions are very nearly normally distributed with only small deviations near the tails. These deviations are slightly more pronounced in the case of the elastic channel.

We now define the summed energy dependent deviation function $\mathscr{D}(E)$ and cross correlation function $C(E)$ as,

$$\mathscr{D}(E)=\frac{1}{N}\sum_{i=1}^{N}D_i(E)\,, \tag{5}$$

$$C(E)=\frac{2}{N(N-1)}\sum_{i>j=1}^{N}D_i(E)D_j(E)\,. \tag{6}$$

The probability density $P(\mathscr{D})$ of $\mathscr{D}$ can be obtained from Eq. (1) by the method of characteristic functions.[20,25] We first calculate the characteristic functions for $D_k(E)$, given by,

$$\phi_k(t)=\int_{-\infty}^{\infty}P_k(D_k)e^{itD_k}dD_k\,, \tag{7}$$

where $P_k(D_k)$ are the probability density functions of $D_k(E)$ calculated using Eq. (1).

The characteristic function of the summed deviation function $\mathscr{D}(E)$ is then given by[24,25]

TABLE I. Values of N_k and Y_{D_k} obtained from the experimental values of $R_k(0)$. Listed are the maximum and minimum values of N_k and the associated values of Y_{D_k} obtained using Eq. (3). The values labeled Mean were used to calculate the theoretical probability distributions used in the comparisons discussed in the text. None of the results are sensitive to this particular choice.

		N_k			Y_{D_k}		
Channel	$R_k(0)$	Min	Mean	Max	Min	Mean	Max
0^+	0.0300	1	1	1	0.985	0.985	0.985
2^+	0.0071	1	2	3	0.996	0.993	0.989
$(2^+,2^+),4^+$ [a]	0.0058	1	6	13	0.997	0.982	0.962
$4^+,2^+$	0.0039	1	12	23	0.998	0.976	0.954
REST	0.00063	1	20[b]		1.000	0.994	

[a]Assumed to be dominated by $2^+,2^+$.
[b]Arbitrarily assumed.

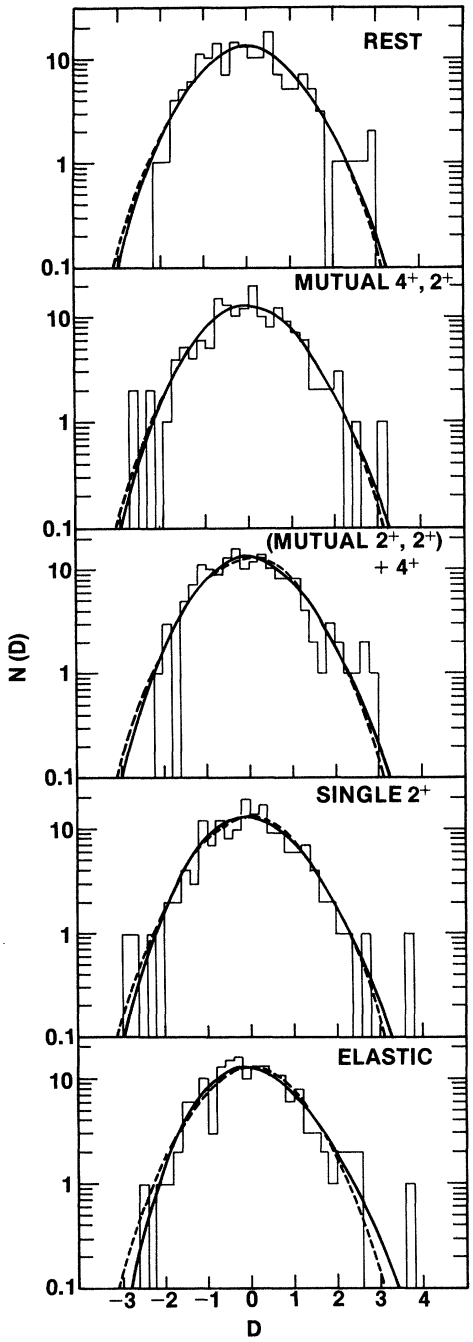

FIG. 4. Frequency distributions of the deviation functions for the five channels. The histogram shows the experimental values. The solid line shows the distributions calculated using Eq. (1) and the values of N_k and Y_{D_k} noted in Table I. The dashed lines show normal distributions.

$$\Phi_{\mathscr{D}}(t)=\prod_{k=1}^{N}\phi_k\left[\frac{t}{N}\right]. \tag{8}$$

The probability density function of $\mathscr{D}(E)$ is then simply given by the Fourier transform[24] of $\Phi_{\mathscr{D}}$,

$$P(\mathscr{D})=\frac{1}{2\pi}\int_{-\infty}^{\infty}\Phi_{\mathscr{D}}(t)e^{-i\mathscr{D}t}dt\ , \tag{9}$$

and can be evaluated by numerical integration. Earlier in this section, we found that $D_k(E)$ are very nearly normally distributed with mean 0 and variance 1. Therefore, for statistically independent $D_k(E)$ normally distributed with distribution functions $P_k(D_k)$, we find that the probability density function $P(\mathscr{D})$ of the summed deviation function $\mathscr{D}$ is a normal distribution with mean 0 and variance σ^2 given by[25]

$$\sigma^2=\frac{1}{N^2}\sum_{i=1}^{N}\sigma_{D_i}^2=0.2\ . \tag{10}$$

The experimental frequency distribution of $\mathscr{D}$ (histogram) and the theoretical predictions (solid curve) are shown in Fig. 5. We have also obtained $P(\mathscr{D})$ by the numerical integration of Eq. (9), using the actual distribution functions $P_k(D_k)$ shown by solid curves in Fig. 4. The distribution function $P(\mathscr{D})$ obtained from this exact calculation has a mean $\mu_{\mathscr{D}}=-0.001$ and variance $\sigma_{\mathscr{D}}^2=0.206$ and is essentially indistinguishable from that calculated assuming normal distributions for $D_k(E)$. The experimental fre-

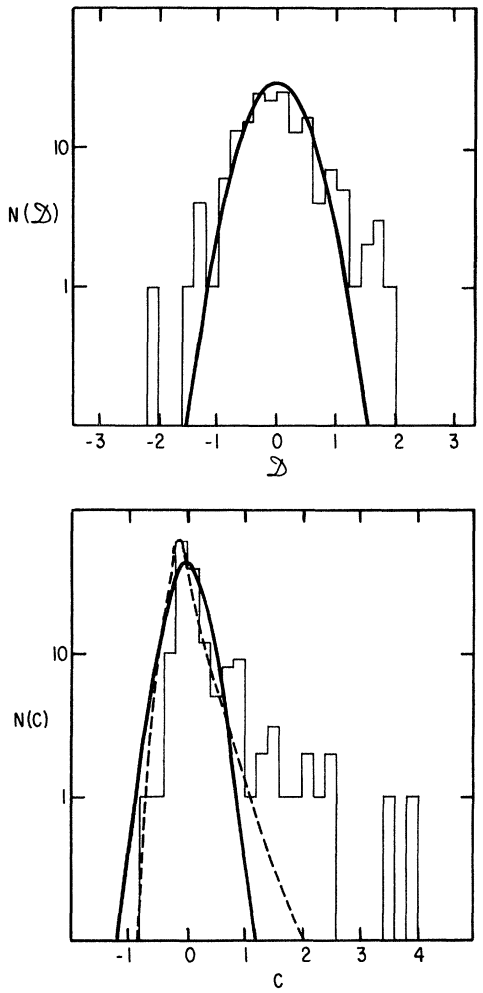

FIG. 5. Frequency distributions for the summed deviation function $\mathscr{D}(E)$ (upper) and cross correlation function $C(E)$ (lower) together with the expected distributions for statistical fluctuations as discussed in the text.

TABLE II. Moments of the experimental and theoretical distributions for $\mathscr{D}(E)$ and $C(E)$. The theoretical values were obtained using different assumptions discussed in the text.

		Fluctuation theory		
Moment	Experiment	Numerical integration	Gaussian	Data
$\mu(\mathscr{D})$	−0.005	−0.001	0.000	
$\sigma^2(\mathscr{D})$	0.429	0.206	0.200	
$\mu_3(\mathscr{D})$	0.080	0.005	0.000	
$\mu(C)$	0.027	0.000	0.002	−0.059
$\sigma^2(C)$	0.470	0.098	0.102	0.077
$\mu_3(C)$	0.839	0.000	0.059	0.020

quency distribution has a mean $\mu_{\mathscr{D}}=0.0$ and variance $\sigma^2_{\mathscr{D}}=0.429$ and has to be compared with the corresponding quantities for the calculated distribution. We observe that $\sigma^2_{\mathscr{D}}(\text{exp})$ is twice as large as $\sigma^2_{\mathscr{D}}(\text{calc})$, indicating that $D_k(E)$ are not statistically independent. These values are summarized in Table II.

To strengthen these conclusions, we calculate the statistical significance limits on $\mathscr{D}$ from the theoretical distribution function $P(\mathscr{D})$. The percentage of data points which are allowed according to the statistical model to have $\mathscr{D}\geq\mathscr{D}_U$ or $\mathscr{D}\leq\mathscr{D}_L$, where $\mathscr{D}_U$ and $\mathscr{D}_L$ are arbitrary upper and lower confidence limits on $\mathscr{D}$, is defined as[25]

$$\alpha=\int_{\mathscr{D}_U}^{\infty}P(\mathscr{D})d\mathscr{D}\ , \tag{11}$$

$$\alpha=\int_{-\infty}^{\mathscr{D}_L}P(\mathscr{D})d\mathscr{D}\ . \tag{12}$$

For a 1% confidence limit $\alpha=0.01$, the values of $\mathscr{D}_U$ and $\mathscr{D}_L$ obtained from Eqs. (11) and (12) are $\mathscr{D}_U=|\mathscr{D}_L|=1.04$. Thus, according to the statistical predictions, the cumulative probability for the events to have $\mathscr{D}\geq\mathscr{D}_U$ or $|\mathscr{D}_L|$ is $2\alpha=0.02$. Therefore, at the most 3 events out of a total of 161 would be expected to lie outside the 1% confidence limits. Contrary to the above prediction, however, we observe from Fig. 5 that at least 13 of the experimentally observed events lie outside the 1% confidence limits, thereby suggesting that the structures observed in the individual channels are strongly correlated.

To make these correlations more apparent, $\mathscr{D}(E)$ is plotted as a function of $E_{\text{c.m.}}$ in Fig. 6(b). Because of the summation over a large number of reaction channels [Eq. (5)], this function tends to average over the statistical fluctuations leaving the correlated structures more apparent. The peaks or dips in $\mathscr{D}(E)$ show one to one correspondence with the structures in the excitation function of TOTAL shown in Fig. 6(a). In Fig. 6(b), the 1% confidence limits are shown by the dashed lines. Evidently most of the peaks or dips in Fig. 6(b) are more than one standard deviation (±0.40) away from the mean value of $\mathscr{D}(E)$. Even under the scrutiny of the more critical test of 1% confidence limits, there are as many as nine structures in Fig. 6(b) which stand out quite prominently, which again signifies the strong correlations among the different channels. These strong correlations indicate a nonstatistical origin for the structures observed in dif-

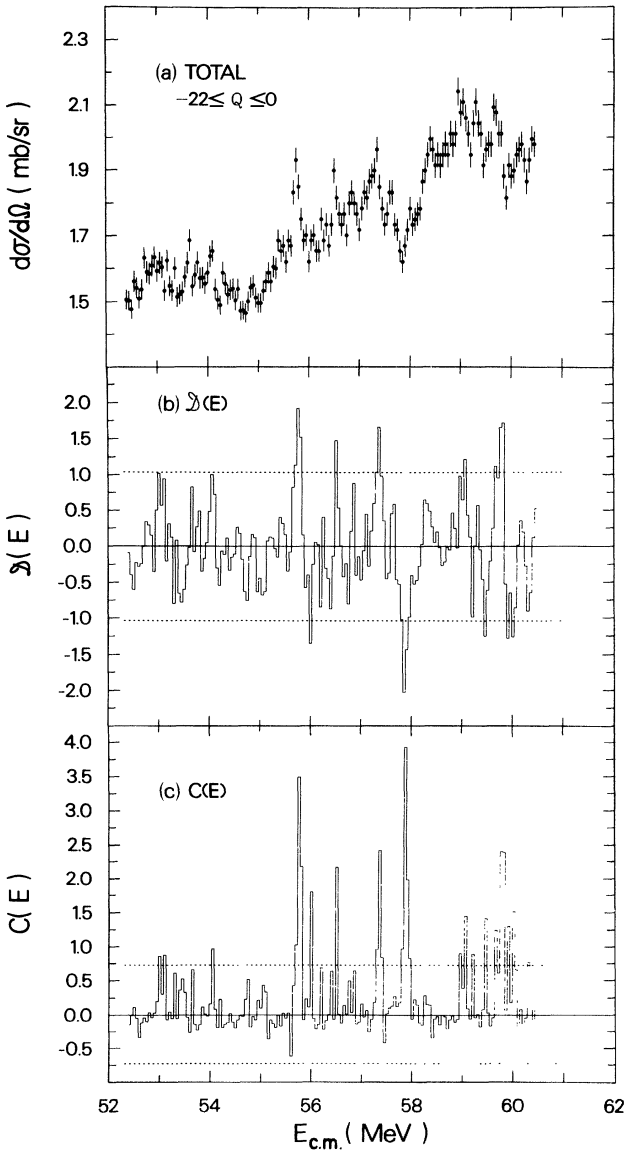

FIG. 6. The summed, angle averaged cross sections (a); summed deviation function $\mathscr{D}(E)$ (b); and cross correlation function $C(E)$ (c) shown plotted versus center-of-mass bombarding energy. The dashed lines in (b) and (c) indicate the 99% confidence limits for statistical fluctuations as discussed in the text.

ferent excitation functions.

We now calculate the theoretical predictions and confidence limits for $C(E)$. Unfortunately, the distribution function $P(C)$ of $C(E)$ cannot be calculated using standard techniques as the terms in the sum [Eq. (6)] which defines $C(E)$ are not strictly statistically independent. We have therefore proceeded in the following three different ways. In the first of these ways, the various terms in the sum of Eq. (6) were assumed to be, in fact, statistically independent, and standard numerical techniques were used to calculate $P(C)$ and the associated confidence limits. Secondly, the $D_k(E)$ were assumed to be normally distributed as discussed above and a Monte Carlo calculation was used to calculate $P(C)$. Lastly, $P(C)$ was calculated using the experimental values of $D_k(E)$ where the values of $D_k(E)$ for each channel were shifted randomly in energy with respect to all the other channels. The values of the moments of the distributions of $C(E)$ obtained using these three procedures are summarized in Table II and the obtained frequency distributions are shown in Fig. 5 for the first method (solid line) and Monte Carlo method (dashed line) together with the experimental frequency distribution.

The experimental cross correlation function $C(E)$ is shown in Fig. 6(c) as a function of $E_{\text{c.m.}}$. Correlations among different channels now manifest themselves as positive peaks [instead of peaks and dips as in the case of $\mathscr{D}(E)$]. As in the case of $\mathscr{D}(E)$, the confidence limits for a nonstatistical character of a particular peak in the cross correlation function $C(E)$ can be obtained from the cumulative distribution function of $P(C)$. The 1% confidence limits on $C(E)$ were calculated to be $C_U = |C_L| = 0.727$ and are shown in Fig. 6(c) by dashed lines. As is evident from Fig. 6(c), most of the peaks in $C(E)$ lie beyond the 1% confidence limits.

The critical tests of summed deviation function and cross correlation function show that the experimental data do not follow the predictions of the statistical model, indicating the existence of strong correlations among structures in different channels. On the basis of the convincing evidence presented in this section, we believe that most of the structures observed in the present data [Figs. 2 and 6(a)] are of nonstatistical origin.

IV. DISCUSSION AND CONCLUSIONS

The statistical fluctuation analysis presented in Sec. III shows the high degree of correlation between the narrow structures observed in the different exit channels. The frequency distribution and confidence limits calculated for the deviation and cross-correlation functions on the basis of the statistical model convincingly demonstrate the nonstatistical origin of these structures. We therefore conclude that they are in fact of resonance origin.

From these data and analyses, together with previous excitation function and angular distribution data,[10] a fairly clear and complete experimental picture emerges. We observe a series of broad structures with width $\Gamma_{\text{c.m.}} \simeq 1$–$2$ MeV which appear not only in the elastic scattering channel but also in the yield summed over many inelastic (and presumably also transfer) channels. Each of these broad structures is fragmented into a number of much narrower resonances with widths $\Gamma_{\text{c.m.}} \simeq 100$–$300$ keV. Measurements of elastic scattering angular distributions in 1 MeV steps over this energy range indicate angular momenta for the broad structures which follow that of the grazing partial wave.[26] Specifically, for the energy range covered in the present data, the three broad structures centered at $E_{\text{c.m.}} = 52.5$, 55.5, and 59 MeV are characterized by angular momenta of $36\hbar$, $38\hbar$, and $40\hbar$, respectively.

These observations then seem to be qualitatively consistent with the picture of the broad structures arising from a series of potential or shape resonances in the entrance channel each of which is fragmented into narrower resonances by mixing with states of a more complex nature. It is extremely unlikely that the narrow resonances we observe correspond to isolated compound nuclear states. For example, $E_{\text{c.m.}} = 59$ MeV corresponds to a compound nucleus excitation energy of 70 MeV which for $J = 40\hbar$ lies some 13 MeV excitation above the rotating liquid drop yrast line.[27] Using a back-shifted Fermi gas level density formula[28] with standard parameters[29] we calculate a compound nucleus level density of 10^4 MeV^{-1} which is several orders of magnitude larger than the observed density of narrow structures. This result suggests that the observed narrow resonances correspond to some special subset of compound nuclear states which, for structural reasons or for reasons of symmetry, are prevented from dissolving into the many times more numerous compound nuclear states.

Some indication of the nuclear structure effects responsible for the obviously small mixing between the resonances and background compound states comes from the partial widths of the resonances for decay into two Si nuclei. If we assume that the $\theta_{\text{c.m.}} = 90°$ cross sections from Ref. 10 arise solely from the resonant amplitudes we obtain values of $\Gamma_{\text{EL}}/\Gamma_{\text{TOT}}$ which are typically a few percent which, together with the observed average widths of ~ 200 keV, leads to a typical value of Γ_{EL} of order 1–2 keV. This is to be compared with the average statistical width[30] of a compound nuclear level for decay into two ^{28}Si nuclei in their ground states of a few eV. We thus see that the resonances have extremely enhanced widths for decay into the ^{28}Si elastic and inelastic channels, an effect which must have its origin in the nuclear structure of the resonances.

Results similar to the above for the ^{12}C+^{12}C system have led to the suggestion and numerous theoretical attempts[12–16] to describe the resonances in terms of nuclear molecular states formed by coupling the rotational degrees of freedom of a dinuclear molecule to the vibrational excitations of the constituent nuclei. To date no such calculations have been performed for the ^{28}Si+^{28}Si system and it is therefore difficult to assess the validity of this approach for the present case. It is true, however, that the observed widths of 200 keV correspond more closely to those expected for compound nuclear states than to resonances in a nuclear molecular potential, and it may therefore be more realistic to attempt to describe the present data in terms of states of an equilibrated compound nucleus which possess a special structure. One possibility along

these lines is that the observed resonances may correspond to extremely deformed shape isomers in the compound nucleus. Calculations[31] within the framework of the Strutinsky prescription do show the existence of well-defined secondary minima for the ^{56}Ni system at large deformations for angular momenta in the vicinity of $40\hbar$. To date, however, there has been no unambiguous experimental demonstration of the existence of such "superdeformed" states in light nuclei and the connection therefore remains tenuous at best. Further experimental and theoretical work is thus essential before any definitive statement can be made regarding the nuclear structure of these narrow high-spin resonances. On the experimental side, it is necessary to obtain more quantitative information on decay widths in the various reaction channels, particularly in channels other than the elastic and inelastic. Some more rigorous spin assignments could be obtained through, for example, phase shift analyses of the elastic scattering data. Theoretically, a more detailed characterization of the expected patterns of decay widths into the elastic, inelastic, and transfer channels as well as estimates of the spreading widths are required. In any case, it is clear that the present observations reflect the existence of states of unusual structure at high excitation energy and angular momentum in a region where it might previously have been thought that nuclear structure effects might long since have vanished.

This work was performed under the auspices of the Office of High Energy and Nuclear Physics, Division of Nuclear Physics, U.S. Department of Energy, under Contract No. W-31-109-ENG-38.

[1]E. Almquist, D. A. Bromley, and J. A. Kuehner, Phys. Rev. Lett. 4, 515 (1960); D. A. Bromley, J. A. Kuehner, and E. Almquist, *ibid.* 4, 365 (1960); Phys. Rev. 123, 878 (1961).

[2]H. Voit, P. Dück, W. Galster, E. Haindl, G. Hartmann, H. E. Helb, F. Silber, and G. Ishenko, Phys. Rev. C 10, 1331 (1974).

[3]D. L. Hansen, R. G. Stokstad, K. A. Erb, C. Olmer, M. W. Sachs, and D. A. Bromley, Phys. Rev. C 9, 1760 (1974).

[4]D. A. Bromley, in *Nuclear Molecular Phenomena,* edited by N. Cindro (North-Holland, Amsterdam, 1978), p. 3, and other contributions therein.

[5]P. Braun-Munzinger, G. M. Berkowitz, T. M. Cormier, C. M. Jachcinski, J. W. Harris, J. Barrette, and M. J. Levine, Phys. Rev. Lett. 38, 944 (1977).

[6]M. R. Clover, R. M. DeVries, R. Ost, N. J. A. Rust, R. N. Cherry, Jr., and H. E. Gove, Phys. Rev. Lett. 40, 1008 (1978).

[7]M. Paul, S. J. Sanders, J. Cseh, D. F. Geesaman, W. Henning, D. G. Kovar, C. Olmer, and J. P. Schiffer, Phys. Rev. Lett. 40, 1310 (1978).

[8]K. R. Cordell, C. A. Weidner, and S. T. Thornton, Phys. Rev. C 23, 2035 (1981).

[9]See contributions in *Resonances in Heavy-Ion Reactions,* edited by K. A. Eberhard (Springer, Berlin, 1982).

[10]R. R. Betts, S. B. DiCenzo, and J. F. Peterson, Phys. Rev. Lett. 43, 253 (1979); Phys. Lett. 100B, 117 (1981).

[11]R. R. Betts, H. G. Clerc, B. B. Back, I. Ahmad, K. L. Wolf, and B. G. Glagola, Phys. Rev. Lett. 46, 313 (1981).

[12]Y. Kondo, Y. Abe, and T. Matsuse, Phys. Rev. C 19, 1356 (1979).

[13]J. Y. Park, W. Greiner, and W. Scheid, Phys. Rev. C 16, 2276 (1976).

[14]O. Tanimura, Nucl. Phys. A309, 233 (1978).

[15]W. A. Friedman, K. W. McVoy, and M. C. Nemes, Phys. Lett. 87B, 179 (1979).

[16]H. Feshbach, J. Phys. Suppl. C 5, 177 (1976).

[17]R. R. Betts, B. B. Back, and B. G. Glagola, Phys. Rev. Lett. 47, 23 (1981); R. R. Betts, in *Resonances in Heavy-Ion Resonances,* edited by K. A. Eberhard (Springer, Berlin, 1982), p. 185.

[18]T. E. O. Ericson and T. Mayer-Kuckuk, Annu. Rev. Nucl. Sci. 16, 183 (1966).

[19]L. C. Dennis, S. T. Thornton, and K. R. Cordell, Phys. Rev. C 19, 777 (1979).

[20]J. Lang, M. Hugi, R. Muller, J. Sromicki, E. Ungricht, H. Witala, L. Jarcyzk, and A. Strzalkowski, Phys. Lett. 104B, 369 (1981).

[21]D. M. Brink and R. O. Stephen, Phys. Lett. 5, 77 (1963).

[22]M. G. Braga Marcazzan and L. Milazzo Colli, Prog. Nucl. Phys. 11, 145 (1970).

[23]A. Ritcher, in *Nuclear Spectroscopy and Reactions, Part B,* edited by J. Cerny (Academic, New York, 1974), p. 343.

[24]*Handbook of Mathematical Functions,* edited by M. Abramowitz and I. A. Stegun (Dover, New York, 1968).

[25]W. Mendenhall and R. L. Schaeffer, *Mathematical Statistics with Applications,* (Duxbury, North Scituate, Massachusetts, 1973).

[26]S. B. DiCenzo, J. F. Petersen, and R. R. Betts, Phys. Rev. C 23, 2561 (1981).

[27]S. Cohen, F. Plasil, and W. J. Swiatecki, Ann. Phys. (N.Y.) 82, 557 (1974).

[28]A. Bohr and B. Mottelson, *Nuclear Structure* (Benjamin, New York, 1969), Vol. I, p. 155.

[29]W. Dilg, W. Schantl, H. Vonach, and M. Uhl, Nucl. Phys. A217, 269 (1973).

[30]J. M. Blatt and V. F. Weisskopf, *Theoretical Nuclear Physics* (Wiley, New York, 1966), p. 389.

[31]M. E. Faber and M. Ploszajczak, Phys. Scr. 24, 189 (1981); (private communication).